Heliyon 8 (2022) e09909

Contents lists available at ScienceDirect

Heliyon

journal homepage: www.cell.com/heliyon

Research article

Long-term L-3-n-butylphthalide pretreatment attenuates ischemic brain injury in mice with permanent distal middle cerebral artery occlusion through the Nrf2 pathway

Mingying Sun [a,b,d,1], Changchun Jiang [a,b,c,1], Xiwa Hao [a,b,c,d], Jiangxia Pang [a,b,c,d], Chao Chen [a,b,c,d], Wenping Xiang [a,b,c], Jun Zhang [a,b,c], Shijun Zhao [a,b,c], Po Wang [a,b,c], Shangyong Geng [a,b,c], Hanzhang Wang [a,b,c], Yuechun Li [a,b,c], Baojun Wang [a,b,c,*]

[a] Department of Neurology, Baotou Central Hospital, Inner Mongolia, China
[b] Neurological Diseases Clinical Medicine Research Center, Inner Mongolia Autonomous Region, China
[c] Cerebrovascular Disease Institute, Inner Mongolia Autonomous Region, China
[d] Neurology Academician Workstation of Baotou Central Hospital, Inner Mongolia, China

HIGHLIGHTS

- Long term preventive administration of NBP could exert a neuroprotective effect on focal cerebral infarction mice models.
- NBP could improve the neurological deficits, reduce infarction size and attenuate the nerve fiber demyelination.
- NBP could promote the nuclear translocation of Nrf2, and up-regulate the expression of HO-1 and NQO1.

ARTICLE INFO

Keywords:
Brain ischemia
L-3-n-butylphthalide
Nrf2 signaling pathway
Oxidative stress
Neuroprotection

ABSTRACT

L-3-n-butylphthalide (NBP), which is used for treatment of mild and moderate acute ischemic stroke, exerts its effects by modulating the Nrf2 pathway. However, it has not been established whether NBP exerts its preventive effects in high-risk ischemic stroke patients through the Nrf2 pathway. We investigated whether NBP exerts its preventive effects through the Nrf2 pathway in long-term NBP pretreated dMCAO mice models. $Nrf2^{+/+}$ wild-type and $Nrf2^{-/-}$ knockout mice were randomized into the vehicle group (equal volume vegetable oil), NBP-low-dose group (20 mg/kg) and NBP-high-dose group (60 mg/kg). The drug was administered once daily by gavage for a month. Then, a permanent distal middle cerebral artery occlusion model (dMCAO) was established after pre-treatment with NBP. Neurological deficits, cerebral infarct volumes, brain water contents, activities of SOD, GSH-Px and MDA levels were determined. Further, axonal injury and demyelination, expression levels of Nrf2, HO-1 and NQO1 in ischemic brains were determined. Long-term NBP pretreatment significantly improved neurological functions, reduced cerebral infarction volumes, reduced brain water contents, increased SOD, GSH-Px activities, decreased MDA contents, reduced neurological injuries, axonal damage as well as demyelination, while increasing Nrf2, HO-1 and NQO1 mRNA as well as protein expressions in dMCAO mice models.

1. Introduction

Cerebral infarction, an acute ischemic cerebrovascular disease is associated with a high morbidity, high disability and high recurrence rates. Globally, stroke is the second leading cause of death, and 87% of stroke-related deaths are caused by ischemic stroke [1, 2]. Intravenous rtPA for recovery of cerebral blood flow is the most effective treatment of ischemic stroke [3, 4]. However, its clinical application is limited by the narrow therapeutic window. Therefore, early prevention of ischemic stroke is important in reducing mortality.

L-3-n-butylphthalide (NBP) is a synthetic small-molecule compound with antioxidant, anti-inflammatory, and protective against mitochondria

* Corresponding author.
E-mail address: jbwwbj@126.com (B. Wang).
[1] The first two authors contributed equally to this paper.

https://doi.org/10.1016/j.heliyon.2022.e09909
Received 15 November 2021; Received in revised form 24 February 2022; Accepted 4 July 2022

and anti-atherosclerotic effects [5]. It is an important neuroprotective drug for the treatment of neurological diseases [6]. NBP exerts its neuroprotective effects by improving energy metabolism and cerebral blood flow [7]. Traumatic brain injury (TBI) mice model experiments have shown that intraperitoneally administered NBP promotes Nrf2 translocation from the cytosol to the nucleus. As a result, it enhances the expressions of Nrf2-antioxidant response elements (AREs) pathway related downstream factors, and increases the activities of antioxidant enzymes, thereby alleviating ischemic brain injury [3].

Nrf2 is an important transcription regulation factor that is widely expressed in mammalian cells. By binding to a stretch of ARE enhancer sequences, it can synergistically induce gene expressions of various antioxidant and detoxifying enzymes [8, 9]. Phase II enzymes include heme oxygenase-1 (HO-1), glutathione-s-transferase (GST) and NAD(P)H quinine oxidoreductase 1 (NQO1) [10]. They constitute a pleiotropic intracellular antioxidant and detoxification defense system, and can scavenge for reactive oxygen species (ROS), reactive nitrogen species (RNS), as well as alleviate cytotoxicity induced by endogenous and exogenous chemical substances. Therefore, these enzymes are involved in maintenance of the intracellular redox potential, thus exerting cytoprotective effects. The Kelch-like ECH-associated protein 1 (Keap1) inhibits Nrf2 nuclear translocation [11]. At physiological conditions, Nrf2 is mainly distributed in the capsulatum, and due to its high-affinity with Keap1, it is maintained at a relatively low level. Cell stimulation by oxidative stress induces the release of Nrf2 from Keap1, its translocation into the nucleus, and its binding to the antioxidant response element (ARE) sequence, thereby initiating the transcription of downstream genes that are then translated to several neuroprotection-associated proteins [12, 13]. Moreover, Nrf2 improves the stability of the atheromatous plaque by modulating gene expressions of γ-glutamylcysteine synthetase (GSH1), HO-1 and NQO1, hence reducing the morbidity and mortality rates of associated diseases. Therefore, for early prevention and treatment of stroke, it is important to design drugs that can up-regulate the expressions of Nrf2 and alleviate oxidative stress.

We used healthy $Nrf2^{+/+}$ and $Nrf2^{-/-}$ male mice in this research. Permanent local cerebral infarction animal models were established via electrocoagulation. Prior to establishment of the animal models, all animals were administered with NBP for 1 month. The effects of NBP on cerebral infarction volume as well as neurological deficits were evaluated, and the role as well as mechanism of NBP in Nrf2 pathway investigated. Our findings provide a basis for timely prevention and treatment of ischemic stroke through antioxidant and neuroprotection.

2. Materials and methods

2.1. Animals

Healthy male $Nrf2^{+/+}$ and $Nrf2^{-/-}$ (ICR background) mice were obtained from the Neurology Laboratory of The Second Hospital of Hebei Medical University [12]. Mice were fed on Co60 sterilized feed (Beijing Keao Xieli Co, Ltd) and provided with purified water. They were housed in an animal laboratory with a constant temperature (20–25 °C) and humidity (75%). During the experiment, all mice were allowed free access to water and food. Male 16-week old mice (25–30 g) were used as controls. The Animal Care and Management Committee of the Second Hospital of Hebei Medical University approved this study (Permit No. HMUSHC-130318). The procedures were performed according to the National Institutes of Health guide for the care and use of Laboratory animals (NIH Publications No. 8023, revised 1978).

2.2. Establishment of cerebral infarction mice models

Cerebral infarction mice models were developed as previously described [12]. Briefly, mice were anesthetized with 10% chloral hydrate (0.35 ml/100 g). Eye ointment was used to lubricate and protect the eyes. Then, mice were fixed in a supine position on an operating table. Routine disinfection using iodine was performed at the center of the neck. An approximately 1 cm median incision was made and the muscle fascia isolated by blunt separation, exposing the right triangle of the neck. The left common carotid artery was isolated and permanently ligated. During the operation, care was taken to avoid damage to the trachea and vagus nerves. Then, a neck skin incision was sewn. Animals were fixed in a left lateral decubitus position and an incision between the right eye and right ear measuring 0.5–1.0 cm made. Carefully, the temporalis muscle was separated outward, exposing the skull bone. A small 2-mm hole was drilled into the skull, exposing the main trunk and branches of the right middle cerebral artery (MCA). The main trunk and branches of MCA were cauterized until the color of the blood vessels changed to white. Flood flow in arterial branches that had been cauterized was assessed by light microscopy, to determine whether the model had been successfully constructed. Muscle tissues were reduced, and the upper skin of the head stitched and sterilized. After operation, mice were housed at 37 °C in a humidity-controlled environment.

2.3. Experimental groups

$Nrf2^{+/+}$and $Nrf2^{-/-}$ mice were randomized into the vehicle group (equal volume vegetable oil), NBP-low-dose group (20 mg/kg) and NBP-high-dose group (60 mg/kg). NBP was dissolved in vegetable oil to a concentration of 30 mg/mL. NBP was orally administered by gavage once daily for 1 month.

2.4. Behavioral assays

2.4.1. Neurological deficit scores

On days 3 and 10 after model establishment, mice were subjected to behavioral analyses in a quiet environment using a modified Longa method (Zhang C et al. 2014). The scoring criteria were: 0: no deficit; 1: contralateral forelimb weakness to stretch; 2: contralateral forelimb flexion; 3: mild turning in circles towards the contralateral side; 4: heavy turning in circles towards the contralateral side; 5: fall to the contralateral side.

2.4.2. The rotarod test

Mice were trained and tested at a fixed time daily in a quiet environment. Before model establishment, all mice were trained on a rotarod cylinder at a constant speed of 4 rpm for 3 days. The inclusion criterion was maintenance of stability for 60 s without falling. On days 3 and 10 after model establishment, all mice underwent the rotarod test at a constant speed of 4 rpm for 60 s. The time from beginning to falling was recorded. The test was performed in triplicates, and the average value calculated.

2.5. Weight changes

Body weights for all mice were recorded daily before and after completion of cerebral infarction model construction.

2.6. Determination of cerebral infarct volumes and brain water contents

On day 10 after model establishment, mice (n = 6, for each group) were anesthetized, decapitated and their brains removed immediately. Starting from the frontal pole, the brains were sliced into 2 mm thick cerebral coronal slices. Brain slices were incubated in 2% triphenyltetrazolium chloride solution (TTC; Sigma) for 10 min at 37 °C, and fixed in 4% paraformaldehyde for 24 h. A normal brain tissue was red whereas the infarct area was white. Brain slices were scanned and analyzed using the Image-Pro Plus 6.0 software. Percentage infarct volumes were calculated as:

$$\text{Infarct volume (\%)} = \{[\text{total infarct volume} - (\text{infarcted hemispheric volume} - \text{infarcted contralateral hemisphere volume})]/\text{infarcted contralateral hemisphere volume}\} \times 100\%$$

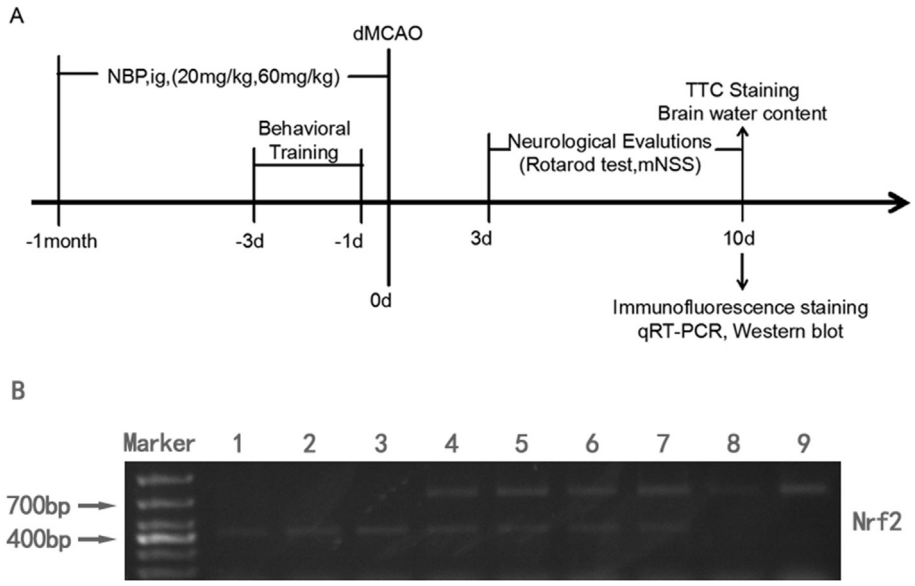

Figure 1. (A) Schematic presentation of the experimental design. (B) Genotypes of Nrf2 as determined by PCR. Mice 1, 2 and 3 were homozygous (1, 2, 3 showed a 400 bp band); mice 4, 5, 6 and 7 were heterozygous (4, 5, 6, 7 showed 2 bands at 400 bp and 750 bp) while mice 8 and 9 were wild-type (8 and 9 showed a 750 bp band).

The dry–wet weight method was used to determine brain water contents. Brain tissues in infarcted regions were isolated, and weighed on a tin foil. Wet weight was the determined weight minus the weight of the tin foil. Brain tissues were wrapped in a tin foil and dried in the oven at 95 °C for 24 h. Tissues were removed from the oven and weighed again. The new weight represented the dry weight. Percentage water content of brain tissues was calculated as:

$$[(wet\ \text{weight}) - (\text{dry weight})] / (wet\ \text{weight}) \times 100\%$$

2.7. Immunofluorescence analysis

On day 10 of model establishment, mice were anesthetized and brain tissues harvested. Tissues were transcardially perfused with saline, followed by 4% paraformaldehyde (PFA) for 24 h. Then, tissues were sequentially dehydrated with 20%, and 30% sucrose. In addition, 30 μm thick coronal sections (LEICA CM1860UV) were obtained. Immunostaining was performed as: Sections were hydrated for 10 min in 0.01 M phosphate buffered saline (PBS pH 7.4), washed thrice using 0.3%Triton-PBS for 5 min, blocked using 1% BSA in PBS for 2 h at room temperature, incubated with primary antibodies and fluorescently tagged with secondary antibodies. After staining, sections were sealed with anti-fluorescence quenching sealing tablets. Immunopositive cells were observed by confocal laser-scanning microscopy (OLYMPUS, Germany). Quantitative analyses were performed using the ImageJ Software. The antibodies used in this study included the Anti-Brdu antibody [IIB5] ab8152 mouse mAb (1:20); Anti-MAP2 antibody [HM-2] ab11267 mouse mAb (1:500); Anti-Myelin Basic antibody [IIB5] ab8152 mouse mAb (1:400); Anti-Neurofilament heavy polypeptide antibody ab8135 rabbit polyclonal (1:400); Donkey Anti-Rabbit IgG H & L (Alexa Fluor®647) ab150075 (1:200) and Goat Anti-Mouse IgG H&L (Alexa Fluor®488) preadsorbed ab150117 (1:200).

2.8. Analysis of Nrf2, HO-1 and NQO1 mRNA expression levels by RT-qPCR

On day 10 after model establishment, mice were anesthetized and decapitated. Immediately, the ischemic sided brain cortices were isolated on ice. Total RNA was extracted by the TRIzol method (TaKaRa, Japan). RNA was reverse-transcribed to cDNA using a reverse transcription kit (TaKaRa, Japan), and samples stored at −80 °C. The primers used in this study were synthesized by Shanghai Bioengineering Company. They were:

Nrf2: F:5′ – GACAAACATTCAAGCCGATTAGAGG-3′,
R:5′- CACATTGGGATTCACGCATAGGA-3′;
NQO1: F: 5′-GGTATTACGATCCTCCCTCAACATC-3′,
R:5′-GAGTACCTCCCATCCTCTCTTCTTC-3′;
HO-1: F: 5′ – TGAATGTACACTCTGGAGATGACAC-3′;
R: 5′-GCTCTGACGAGTGACGCTATCTGT-3′;
GAPDH: F: 5′-TGAACGGGAAGCTCACTGG-3′;
R: 5′-GCTTCACCACCTTCTTGATGTC-3′.

Nrf2, HO-1 and NQO1 mRNA expression levels were determined by real-time quantitative real-time polymerase chain reaction. Relative gene expression levels were determined by the 2-ΔCt method.

2.9. Evaluation of Nrf2, HO-1 and NQO1 protein levels in ischemic brain tissues

On day 10, mice were anesthetized, decapitated and their brains removed immediately. Ischemic sided brain cortices were immediately isolated in ice, placed into 1.5 ml tubes and stored at −80 °C. Fifty grams of brain tissues from the ischemic side were used for extraction of total proteins using a total protein extraction kit (Biyuntian Biotechnology Co, Ltd, Shanghai, China). Protein concentrations were determined using a BCA Kit (Thermo Fisher Scientific). Nrf2, HO-1 and NQO1 protein levels in ischemic sided brain cortices were determined by Western blotting. Approximately 30 ug of the total protein was separated by SDS-polyacrylamide gel electrophoresis (SDS-PAGE) and transferred onto PVDF membranes, which were blocked with 10% bovine serum albumin (BSA, diluted with 0.01 mmol/L phosphate-buffered saline) at room temperature for 1 h. Then, the following antibodies were separately added: Nrf2 Rabbit polyclonal antibody (1:1000 Abcam), NQO1 Rabbit Monoclonal antibody (1:1000 ab80588 Abcam), HO-1 Rabbit Monoclonal antibody (1:2000 ab52947 Abcam), and β-actin Rabbit polyclonal antibody (1:5000 20536-1-AP Abcam) after which overnight incubation was performed at 4 °C on a shaker. Then, the PVDF membrane was washed thrice (10 min each time) using TBST. The second antibody, Goat anti-rabbit IgG H&L (HRP) ab205718 (Abcam 1:2000) was added and incubated for 1 h on a shaker at room temperature. The PVDF membrane was again washed thrice (10 min each time) using TBST after which it was stained using an ECL luminescent solution and analyzed under an infrared imaging system (Bio-Rad, USA).

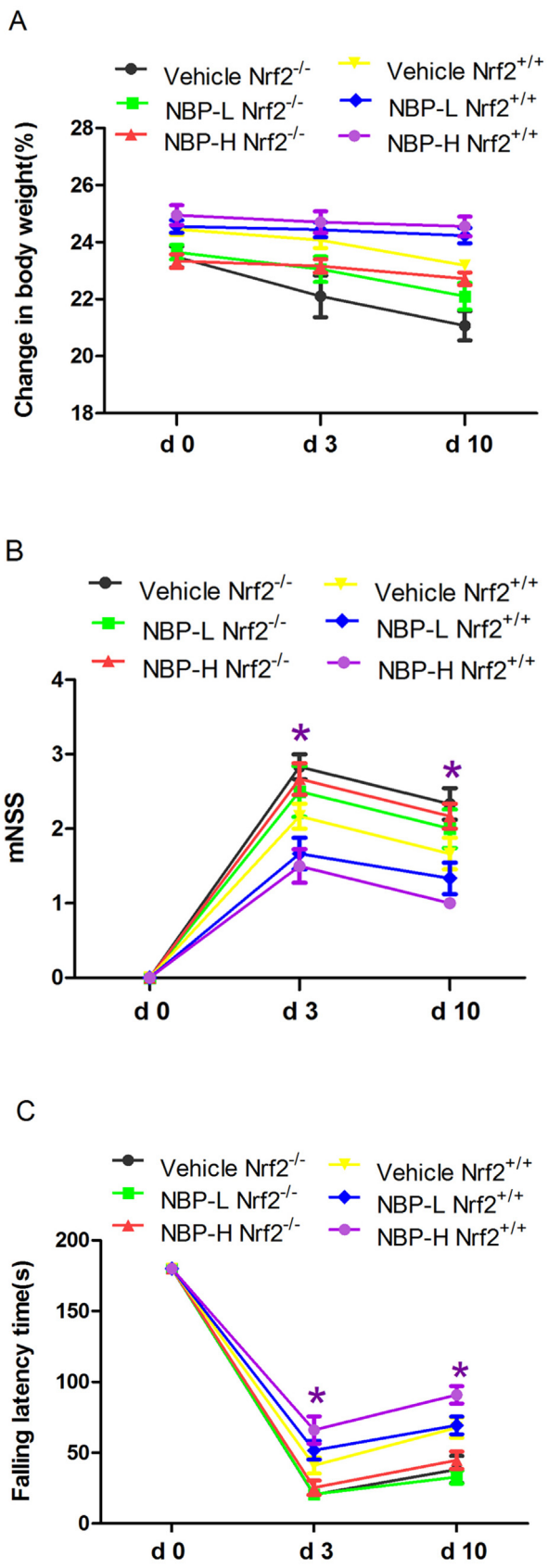

Figure 2. Effects of NBP on body weights and neurological deficits. (A) Changes in body weights were determined during the whole experimental procedure. (B and C) mNSS evaluation and Rotarod tests were performed on days 3 and 10. Data are expressed as mean ± SEM, n = 6, [a]$Nrf2^{+/+}$ high-dose group vs control group, *$p < 0.05$; [b]$Nrf2^{+/+}$ control group vs $Nrf2^{-/-}$ control group, *$p < 0.05$.

3. Statistical analysis

SPSS10.0 was used for statistical analyses. All data are expressed as means ± SD. One-way analysis of variance (ANOVA) followed by the Tukeys post-hoc test were used for comparisons among multiple groups. $p \leq 0.05$ was the threshold for statistical significance.

4. Results

4.1. The Nrf2 mice genotypes

F1 mice genotypes are presented in Figure 1B. Mice 1, 2 and 3 mice were homozygous (1, 2, 3 showed a 400 bp band); 4, 5, 6 and 7 were heterozygous (4, 5, 6, 7 showed 2 bands, at 400 bp and 750 bp) while mice 8 and 9 were wild-type strains (8, 9 showed a 750 bp band). This results prove that NBP had no significant effect on weight in $Nrf2^{+/+}$ and $Nrf2^{-/-}$ mice.

4.2. NBP improved the neurological deficits in $Nrf2^{+/+}$ mice but not $Nrf2^{-/-}$ mice

4.2.1. Body weight changes

On days 3 and 10 day after model establishment, there was a progressive decrease in body weights for all groups. However, differences in body weights between groups were insignificant (Figure 2A). Differences between weights of mice in the NBP-high-dose group and mice in the NBP-low-dose group were significant (Figure 2A).

4.2.2. Neurological deficit scores

Compared to the vehicle group, there were marked differences in neurological deficit scores of $Nrf2^{+/+}$ mice in the NBP-high-dose group on days 3 and 10 after model development ($p < 0.05$, Figure 2B). However, there were no significant differences in neurological deficit scores between $Nrf2^{-/-}$ mice in the NBP-high-dose group and NBP-low-dose group (Figure 2B). Between group comparisons of $Nrf2^{+/+}$ and $Nrf2^{-/-}$ mice at different time points within the same dose showed that only $Nrf2^{+/+}$ mice in the NBP-high-dose group had significantly different neurological severity scores over time ($p < 0.05$, Figure 2B). However, the other groups exhibited a decrease in neurological scores. At the same time point, neurological deficit scores for $Nrf2^{+/+}$ mice in the NBP-high-dose group were significantly different, compared to the other groups ($p < 0.05$, Figure 2B). On days 3 and 10 day after model development, there were significant differences between $Nrf2^{+/+}$ mice and $Nrf2^{-/-}$ mice in the vehicle group ($p < 0.05$, Figure 2B).

4.2.3. Rotarod test results

Rotarod test results of $Nrf2^{+/+}$ mice in the NBP-high-dose group were significantly different compared to NBP-low-dose and vehicle groups ($p < 0.05$, Figure 2C). Rotarod test results for $Nrf2^{-/-}$ mice in the NBP-high-dose group did not reveal significant differences, compared to the NBP-low-dose group (Figure 2C). Analysis of $Nrf2^{+/+}$ and $Nrf2^{-/-}$ mice at different time points within the same dose showed that only the $Nrf2^{+/+}$ mice in the NBP-high-dose group had significantly different rotarod test scores over time ($p < 0.05$, Figure 2C). Notably, the other groups exhibited a decrease in rotarod test scores (Figure 2C). Between group comparisons at different dose groups within the same time point showed that only the $Nrf2^{+/+}$ mice in the NBP-high-dose group had significant differences in rotarod test scores among different doses ($p < 0.05$, Figure 2C). There were significant differences in rotarod test scores for $Nrf2^{+/+}$ mice in the vehicle group, compared to $Nrf2^{-/-}$ mice in the vehicle group ($p < 0.05$, Figure 2C).

4.3. NBP reduced the brain infarction volumes in $Nrf2^{+/+}$ mice but not $Nrf2^{-/-}$ mice

The cerebral cortex area infarct volume for the $Nrf2^{+/+}$ vehicle group was significantly smaller compared to that of the $Nrf2^{-/-}$ vehicle group

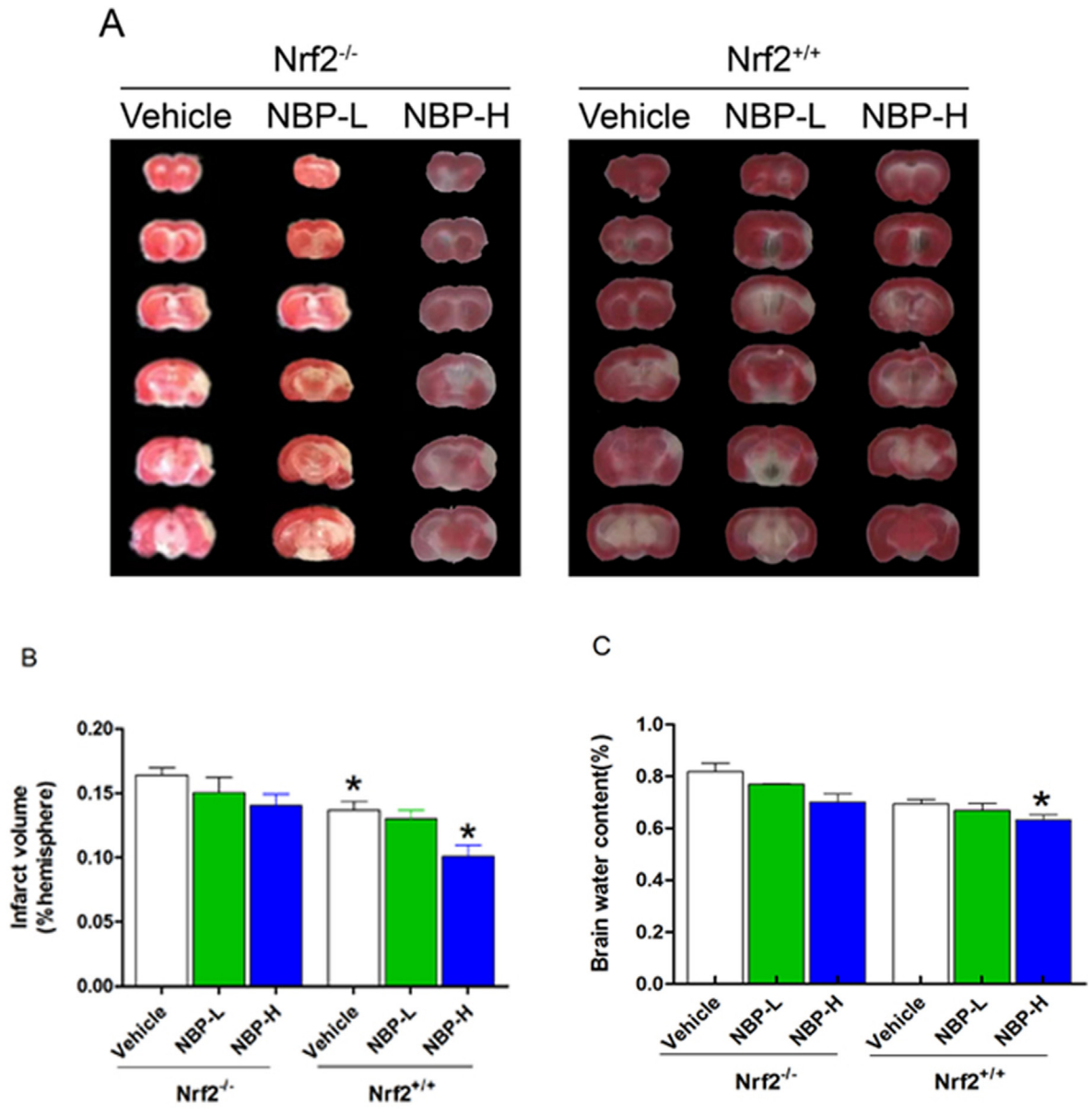

Figure 3. Effects of NBP on brain water contents and brain infarction volumes. (A) Representative images of TTC staining on day 10. (B) Quantification of brain infarction volumes on day10. (C) Quantification of brain water contents on day10. Data are expressed as mean ± SEM, n = 6, [a]$Nrf2^{+/+}$ high-dose group vs control group, *$p < 0.05$; [b]$Nrf2^{+/+}$ control group vs $Nrf2^{-/-}$ control group *$p < 0.05$.

(Figure 3A-B, $p < 0.05$). The cerebral cortex area infarct volume for $Nrf2^{+/+}$ mice decreased with increasing NBP concentrations. The cerebral cortex area infarct volume for the NBP-high-dose group was significantly low, compared to the vehicle group (Figure 3A-B, $p < 0.05$). The cerebral cortex area infarct volume for the $Nrf2^{-/-}$ mice decreased with increasing NBP concentrations. However, there were no significant differences among groups (Figure 3A-B). Brain water contents decreased with increasing NBP doses. Notably, $Nrf2^{+/+}$ mice in the NBP-high-dose group showed significant differences across different doses ($p < 0.05$, Figure 3C).

4.4. NBP improved the tissue loss in $Nrf2^{+/+}$ mice

MAP2 immunostaining was used to analyze the tissue loss. The number of MAP2 positive cells was counted by imageJ, and the more MAP2 positive cells were, the more seriously the neuronal damage. Neuronal injury in the $Nrf2^{+/+}$ NBP-high-dose group was significantly decreased, compared to the $Nrf2^{+/+}$vehicle group ($p < 0.05$, Figure 4B-C). The $Nrf2^{-/-}$ NBP-high-dose group and NBP-low-dose group showed relative alleviations in neuronal deficits, compared to the $Nrf2^{-/-}$ vehicle group, however, the difference was not significant (Figure 4A–C). There was a decrease in MAP2 positive staining of $Nrf2^{+/+}$ mice, smaller infarct sizes, and neuronal injury was less, compared to $Nrf2^{-/-}$ mice in the vehicle group ($p < 0.05$, Figure 4A–C).

4.5. NBP decreased the axonal damage and demyelination in the peri-infarct area

Ischemic stroke is attributed to oligodendrocyte damage, leading to axonal myelin loss. The characteristics of axonal myelin loss include SMI-32 positive staining and MBP negative staining. The effects of NBP on axonal damage were comparable to those on neuronal damage. The levels of SMI-32 positive staining of the cerebral infarct mice decreased with increasing NBP doses, whereas the level of MBP positive staining increased with increasing NBP doses, and $SMI\text{-}32^{+}/MBP^{+}$ decreased with increasing NBP doses, compared to the $Nrf2^{+/+}$ vehicle group, However,

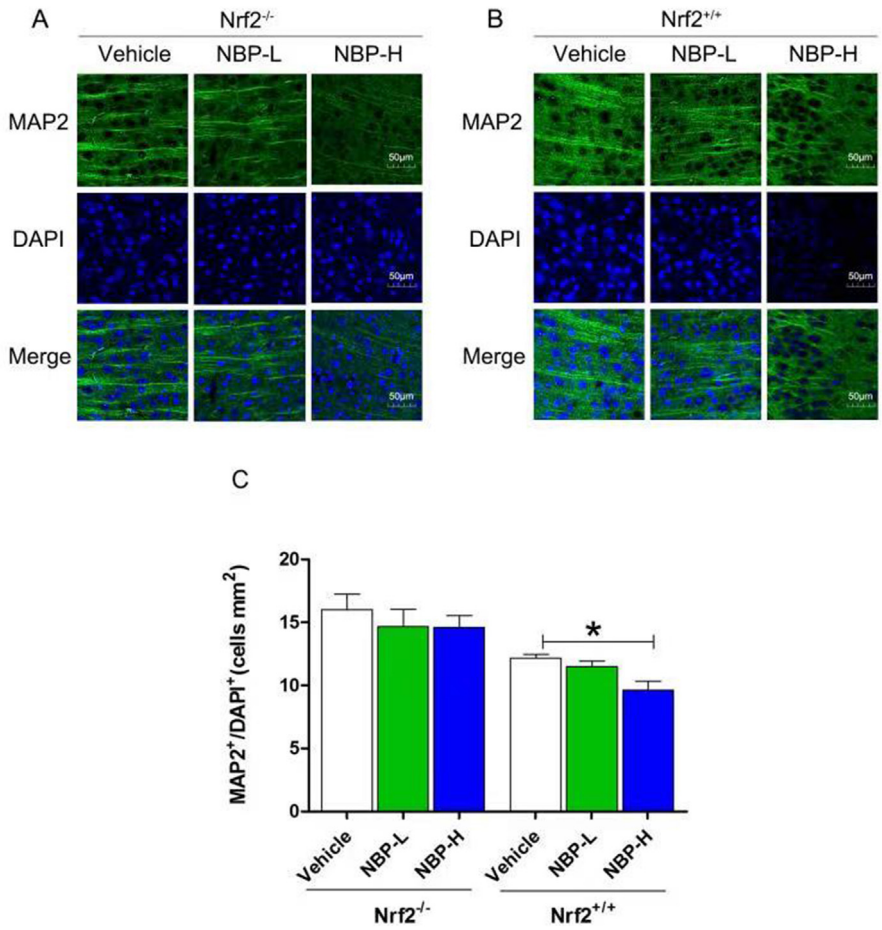

Figure 4. Effects of NBP on neurological injury on day 10. (A and B) Representative images showing MAP2 (green) and DAPI (blue) double-immunostaining of ischemic area of $Nrf2^{-/-}$ and $Nrf2^{+/+}$ mice. Scale bars = 22 μm. (C) Quantification of Figure 5A and Figure 5B n = 6, [a]$Nrf2^{+/+}$ high-dose group vs control group, $*p < 0.05$; [b]$Nrf2^{+/+}$ control group vs. $Nrf2^{-/-}$ control group, $*p < 0.05$.

only the $Nrf2^{+/+}$ NBP- high-dose group exhibited significant differences across dosages ($p < 0.05$, Figure 5B-C). All drug intervention groups with $Nrf2^{-/-}$ mice exhibited a downward trend compared to the vehicle group, however, the difference was not significant (Figure 5A–C). The $Nrf2^{+/+}$ mice in the vehicle group SMI-32^{+}/MBP^{+} showed a significant decrease trend compared to Nrf2−/− mice vehicle group ($p < 0.05$, Figure 5A–C).

4.6. NBP increased the Nrf2, HO-1 and NQO1 mRNA expression levels in $Nrf2^{+/+}$ mice but not $Nrf2^{-/-}$ mice levels

In order to study the effect of NBP on the Nrf2 pathway, the Nrf2, HO-1 and NQO1 mRNAs were extracted from the ischemic brain cortex and measured the corresponding mRNA levels by RT-qPCR. Nrf2, HO-1 and NQO1 mRNA levels for $Nrf2^{+/+}$ mice in the vehicle group were significantly higher, compared to $Nrf2^{-/-}$ mice in the vehicle group (Figure 6A–C, $p < 0.05$). The Nrf2, HO-1 and NQO1 mRNA levels for $Nrf2^{+/+}$ mice increased with increasing NBP dose, and all intergroup comparisons exhibited significant differences ((Figure 6A–C, $p < 0.05$). The mRNA levels for Nrf2, HO-1 and NQO1 in the $Nrf2^{-/-}$ drug intervention groups did not exhibit significant differences, compared to levels in the vehicle group.

4.7. NBP activated the Nrf2 pathway in $Nrf2^{+/+}$ mice

To further verify the effect of NBP on the Nrf2 pathway, we extracted the proteins from the ischemic brain cortex and measured the corresponding protein levels by Western blotting. HO-1, nucleus-Nrf2 and cytoplasm-Nrf2 protein levels were significantly high in the $Nrf2^{+/+}$ vehicle group, compared to levels in the $Nrf2^{-/-}$ vehicle group (Figure 7A-B-C, $p < 0.05$). Protein levels of HO-1 and NQO1 for $Nrf2^{+/+}$ mice in drug groups were significantly high, compared to vehicle $Nrf2^{+/+}$ group (Figure 7C-D, $p < 0.05$). Moreover, HO-1 (Figure 7C, $p < 0.05$) and NQO1 (Figure 7D, $p < 0.01$) protein levels for mice in the NBP-high-dose group were significantly high, compared to those of the NBP-low-dose group. Protein levels of nucleus-Nrf2 increased with increasing NBP doses, however, cytoplasm-Nrf2 protein levels decreased with increasing NBP doses. Notably, differences between groups were significant (Figure 7A-B, $p < 0.05$). The Nrf2, HO-1 and NQO1 protein levels for $Nrf2^{-/-}$ mice in drug groups were not significantly different, compared to protein levels for $Nrf2^{-/-}$ mice in the vehicle group. Taken together, we verified that NBP promoted the protein expression levels of HO-1 and NQO1 by activating the Nrf2 pathway in $Nrf2^{+/+}$ mice.

5. Discussion

The focal cerebral infarction model can be established by electrocoagulation. It is characterized by neuronal cell death, local inflammatory activation, and blood brain barrier damage, resulting in cerebral cortex infarction, smaller cortical infarct sizes and increased survival time. Therefore, the animal model is extensively used in ischemic stroke studies [14]. In this study, before establishing the model, animals were subjected to prophylactic NBP drug pre-treatment for a month. There was a significant decrease in neurological deficits for $Nrf2^{+/+}$ mice in the NBP-high-dose group. This outcome was attributed to alleviation of ischemic stroke-induced neurological deficits by NBP through microcircuit reconstruction, mitochondrial protection, reduction of ischemia-induced

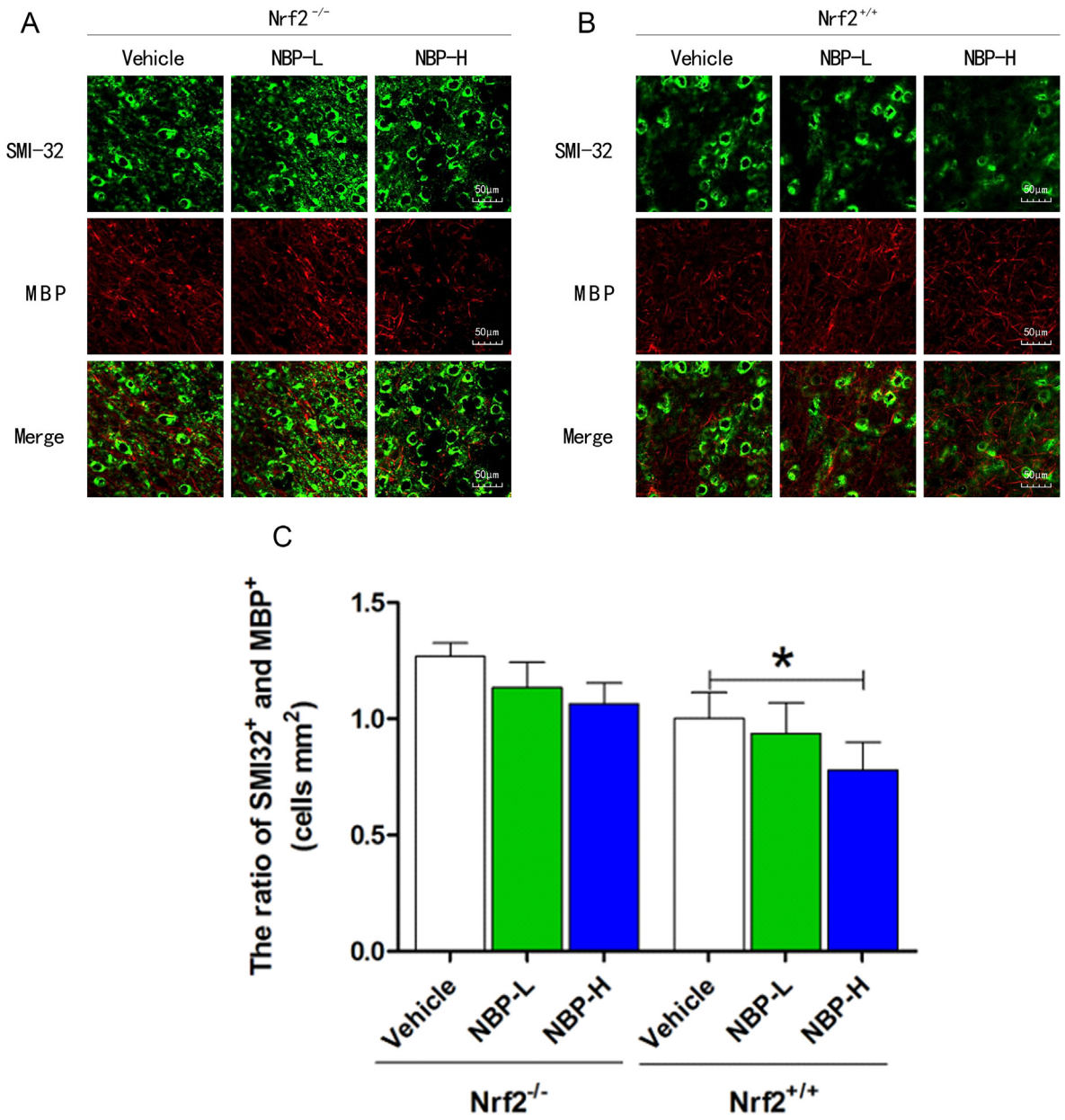

Figure 5. NBP decreased axonal damage and demyelination on day 10. (A and B) Representative images showing SMI-32 (green) and MBP (red) double-immunostaining in ischemic area of $Nrf2^{-/-}$ and $Nrf2^{+/+}$ mice. Scale bars = 22 μm. (C) Quantification of A and B. n = 6, $^{a}Nrf2^{+/+}$ high-dose group vs control group, $^{*}p < 0.05$; $^{b}Nrf2^{+/+}$ control group vs. $Nrf2^{-/-}$ control group, $^{*}p < 0.05$.

neuronal apoptosis, and inhibition of inflammatory responses induced by oxidative stress [6]. Brain cortex infarction volumes for $Nrf2^{+/+}$ mice in the NBP-high-dose group significantly decreased after NBP treatment. Possibly, NBP exerts its effects through antiplatelet aggregation, attenuation of oxidative stress injury-induced cerebral ischemia, regulation of energy metabolism, and amelioration of microcirculation, thereby reducing the infarct sizes [7]. Moreover, NBP-low-dose (20 mg/kg) showed significant neuroprotective effects in this study. A previous study reported that NBP (40–160 mg/kg) pre-treatment reduces inflammation in injured brains, whereas 20 mg/kg NBP did not show significant neuroprotective effects. The difference in activities may have been because of the low NBP concentrations (20 mg/kg), which may have been insufficient to upregulate the expressions of protection-associated factors, thereby antagonizing the ischemia-induced brain damage [11].

The main causes of oligodendrocyte death and demyelination in the central nervous system include trauma, ischemia, autoimmune attacks or inflammation, and ischemic stroke causes inflammation [15, 16]. Therefore, ischemic stroke can cause oligodendrocyte damage and axonal demyelination, thus affecting the normal functions of neurons. The remyelination process involves the proliferation and differentiation of oligodendrocyte progenitor cells into myelin oligodendrocytes [17, 18]. Oligodendrocytes, which are mainly found in the central nervous system, have a vital role in remyelination after injury. They wrap around axons to form an insulating myelin sheath structure, which is involved in smooth transmission of bioelectric signals and promotes normal neuronal functions. Abnormalities in oligodendrocytes are associated with nerve fiber demyelination [19]. The main cause of oligodendrocyte death in the central nervous system is the demyelinating diseases [20]. The most common demyelinating disease is multiple sclerosis, which is characterized by immune-mediated attacks on myelin and oligodendrocytes caused by myelin-specific $CD8^{+}$T cells, leading to the destruction of myelin and death of oligodendrocytes [21, 22], inducing axons to peel off

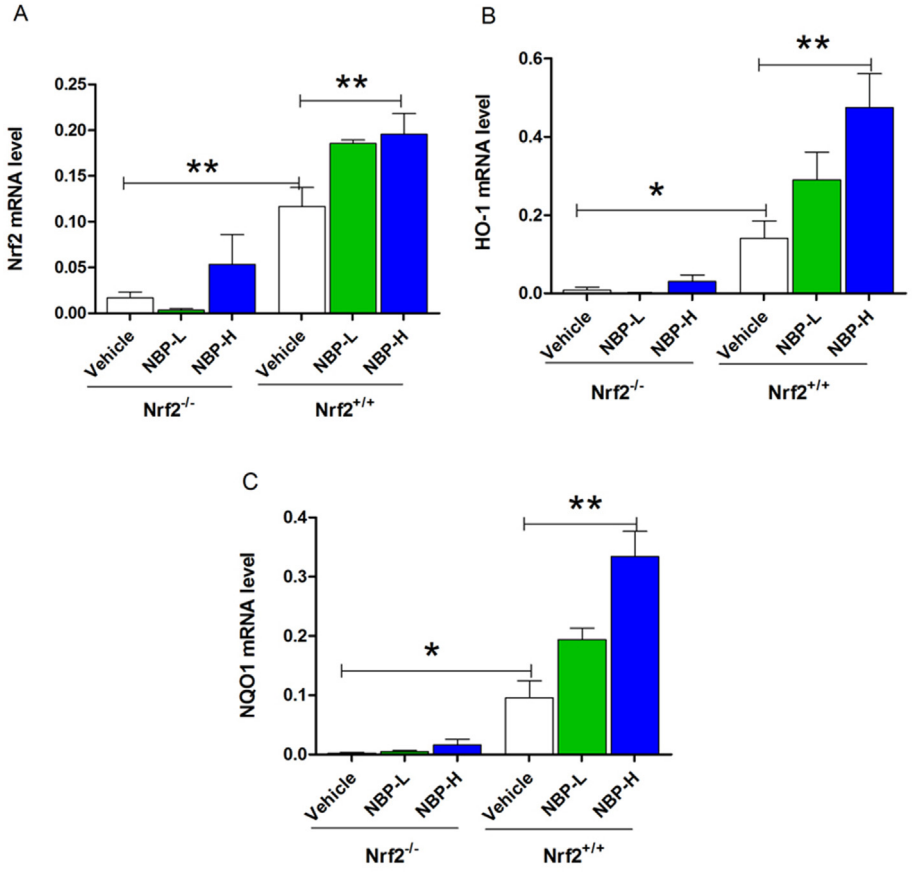

Figure 6. Effects of NBP on Nrf2, HO-1 and NQO1 mRNA levels. (A, B and C) Quantification of Nrf2, HO-1 and NQO1 mRNA expressions on day 10. Data are expressed as mean ± SEM, n = 6, [a]$Nrf2^{+/+}$ high-dose group vs control group, *$p < 0.05$; [b]$Nrf2^{+/+}$ control group vs. $Nrf2^{-/-}$ control group *$p < 0.05$.

and promote neurodegeneration [23]. Therefore, remyelination is highly correlated with oligodendrocytes, and both are implicated in ischemia-induced brain damage. NBP inhibits the release of pro-inflammatory factors, promotes oligodendrocyte proliferation and differentiation, and promotes myelin regeneration to replenish damaged myelin [18]. MBP is an important mature oligodendrocyte marker. SMI-32 is a marker for dephosphorylated nerve fibers that are implicated in axonal damage. Ischemic stroke causes oligodendrocyte damage and axonal myelination barriers. Ischemic stroke is characterized by increased SMI-32 positive staining and decreased MBP positive staining, implying an increased ratio of $SMI\text{-}32^{+}/MBP^{+}$. We established that $Nrf2^{+/+}$ mice in the NBP-high-dose group had significantly low $SMI\text{-}32^{+}/MBP^{+}$ ratios, compared to the vehicle group. Notably, the $Nrf2^{-/-}$ mice in the drug-treated groups exhibited a decreased $SMI\text{-}32^{+}/MBP^{+}$ ratio, compared to the vehicle group, however, the difference was not significant. These findings indicate that long-term pre--treatment with NBP for cerebral infarction decreases oligodendrocyte damage and demyelination of axons through the Nrf2 signaling pathway.

Nrf2 is a basic leucine zipper transcription factor that is inhibited by Keap1 [24]. Under oxidative stress conditions, Nrf2 is released from the Keap1 inhibitory complex and translocated into the nucleus, thereby binding antioxidant response elements (AREs). After binding AREs, Nrf2 up-regulates the expressions of target genes, such as glutamate-cysteine ligase, glutathione peroxidase (GSH-Px), heme oxygenase (HO-1) and NAD(P)H: quinone oxidoreductase I (NQO1). These genes exert cyto-protective effects by scavenging for oxygen radicals and peroxide as well as maintaining an intracellular redox state [25]. The findings of this study showed that Nrf2 protein levels for $Nrf2^{+/+}$ mice in the NBP-high-dose group were higher in the nucleus, whereas protein levels of Nrf2 in the cytoplasm were low. This finding implies that NBP promotes the activation of Nrf2 and its translocation into the nucleus. Moreover, NBP treatment increased the mRNA and protein levels of HO-1 and NQO1, implying that NBP upregulated the expressions of Nrf2 and downstream antioxidant stress genes, thereby exerting neuroprotective effects.

Experimentally, HO-1 overexpression decreases the volume of cerebral infarction [26]. Cerebral infarct volume for HO-1 knockout mice was significantly large, compared to wild-type mice [27]. NQO1 is a ubiquitous phase II detoxification enzyme whose expression levels are high in the nervous system. NQO1 has a major role in the detoxification of exogenous toxicants. It exerts its strong anti-oxidant effects by reducing the levels of endogenous quinones and inactivating endogenous prooxidants [28]. HO-1 and NQO1 are important downstream target genes of the Nrf2 signaling pathway. In this study, the cerebral cortex infarct volume size for $Nrf2^{+/+}$ mice in the vehicle group was significantly low, compared to $Nrf2^{-/-}$ mice in the vehicle group. Thus, Nrf2 has a neuroprotective effect during the early phase of ischemic brain injury. NQO1 and HO-1 levels for $Nrf2^{+/+}$ mice in NBP-high-dose group were markedly increased, while the infarct volume and brain edema were significantly attenuated. In addition, neurological deficits of $Nrf2^{+/+}$ mice in the NBP-high-dose group were significantly improved. This implies that NBP improves ischemic brain injury during the early phase of cerebral infarction, and exerts its neuroprotective effects through antioxidant and anti-inflammatory effects. On the contrary, NQO1 and HO-1 levels for $Nrf2^{-/-}$ mice in the NBP-high-dose group did not show significant differences, compared to the vehicle group. In addition, the infarct volume of $Nrf2^{-/-}$ mice did not show significant reduction, and neurological deficits were not significantly improved. This implies that protective effects of NBP on ischemic brain tissues were not significant.

In summary, NBP improves neurological deficits, reduces infarct sizes, decreases brain edema, and attenuates nerve fiber demyelination as

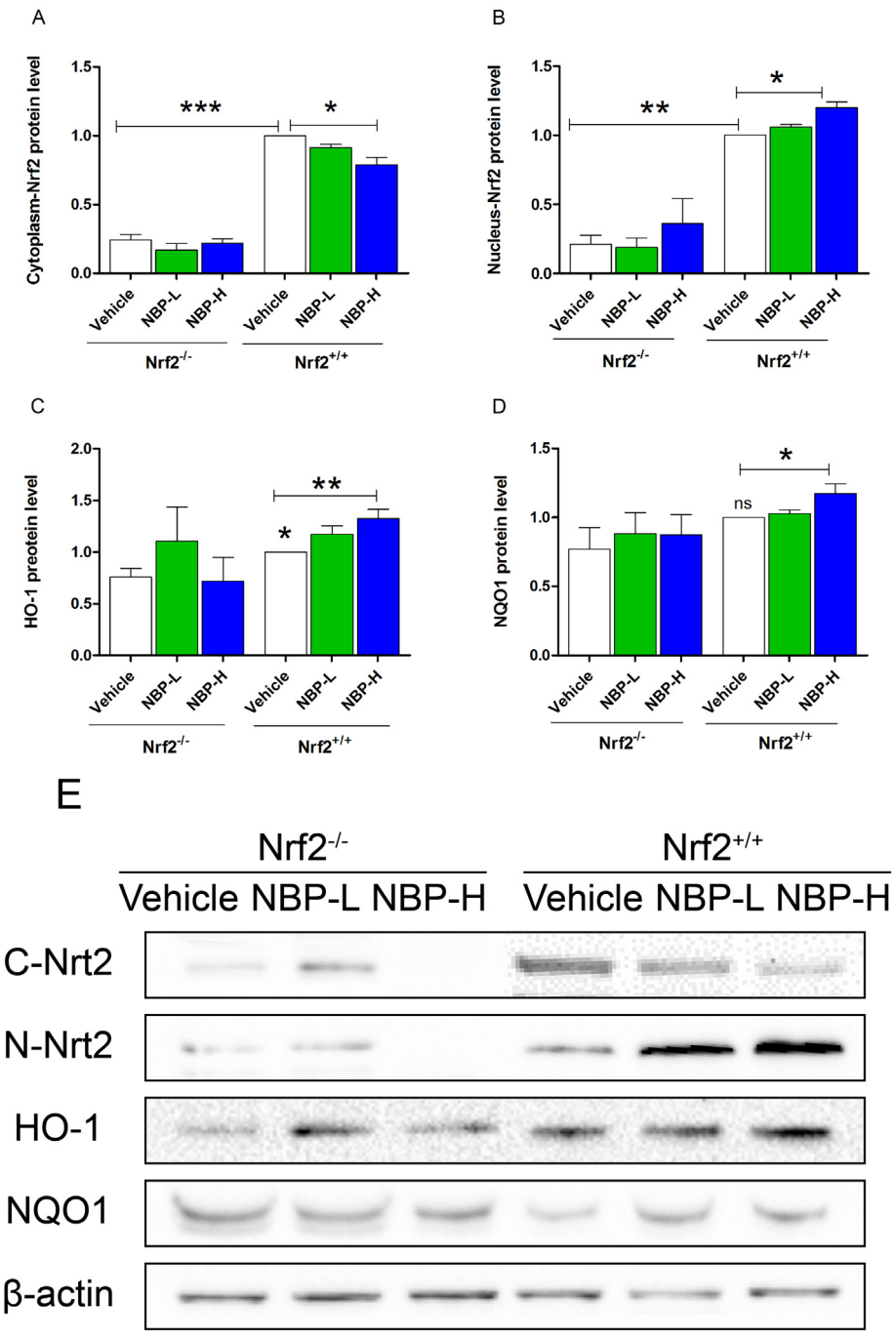

Figure 7. Effects of NBP on Nrf2, HO-1 and NQO1 protein levels. (A and B) cytoplasm-Nrf2 and nucleus-Nrf2 protein levels on day10. (C and D) HO-1 and NQO1 protein levels on day10. (E) cytoplasm-Nrf2, nucleus-Nrf2, HO-1 and NQO1protein levels on day10. Data are expressed as mean ± SEM, n = 6, [a]$Nrf2^{+/+}$ high-dose group vs control group, *$p < 0.05$; [b]$Nrf2^{+/+}$ control group vs. $Nrf2^{-/-}$ control group *$p < 0.05$.

well as axonal damage by promoting nuclear translocation of Nrf2 and expressions of its downstream antioxidant stress factors, including HO-1 and NQO1.

Declarations

Author contribution statement

Mingying Sun: Performed the experiments; Analyzed and interpreted the data; Wrote the paper.

Changchun Jiang: Conceived and designed the experiments; Performed the experiments; Analyzed and interpreted the data; Wrote the paper.

Xiwa Hao: Conceived and designed the experiments; Performed the experiments; Wrote the paper.

Jiangxia Pang: Conceived and designed the experiments; Performed the experiments; Contributed reagents, materials, analysis tools or data.

Chao Chen; Wenping Xiang: Conceived and designed the experiments; Performed the experiments; Analyzed and interpreted the data.

Jun Zhang; Hanzhang Wang & Po Wang: Performed the experiments; Analyzed and interpreted the data.

Shijun Zhao; Shangyong Geng: Performed the experiments; Analyzed and interpreted the data; Contributed reagents, materials, analysis tools or data.

Yuechun Li: Conceived and designed the experiments; Analyzed and interpreted the data; Contributed reagents, materials, analysis tools or data.

Baojun Wang: Conceived and designed the experiments; Analyzed and interpreted the data; Wrote the paper.

Funding statement

Changchun Jiang was supported by Natural Science Foundation of Inner Mongolia [2019MS08206].

Data availability statement

Data will be made available on request.

Declaration of interest's statement

The authors declare no conflict of interest.

Additional information

Supplementary content related to this article has been published online at https://doi.org/10.1016/j.heliyon.2022.e09909.

References

[1] E.J. Benjamin, S.S. Virani, C.W. Callaway, A.M. Chamberlain, A.R. Chang, S. Cheng, S.E. Chiuve, M. Cushman, F.N. Delling, R. Deo, S.D. de Ferranti, J.F. Ferguson, M. Fornage, C. Gillespie, C.R. Isasi, M.C. Jimenez, L.C. Jordan, S.E. Judd, D. Lackland, J.H. Lichtman, L. Lisabeth, S. Liu, C.T. Longenecker, P.L. Lutsey, J.S. Mackey, D.B. Matchar, K. Matsushita, M.E. Mussolino, K. Nasir, M. O'Flaherty, L.P. Palaniappan, A. Pandey, D.K. Pandey, M.J. Reeves, M.D. Ritchey, C.J. Rodriguez, G.A. Roth, W.D. Rosamond, U.K.A. Sampson, G.M. Satou, S.H. Shah, N.L. Spartano, D.L. Tirschwell, C.W. Tsao, J.H. Voeks, J.Z. Willey, J.T. Wilkins, J.H. Wu, H.M. Alger, S.S. Wong, P. Muntner, E. American Heart Association Council on, C. Prevention Statistics, S. Stroke Statistics, Heart disease and stroke statistics-2018 update: a report from the American heart association, Circulation 137 (2018) e67–e492.

[2] V.L. Feigin, B. Norrving, G.A. Mensah, Global burden of stroke, Circ. Res. 120 (2017) 439–448.

[3] Z. Liu, H. Wang, X. Shi, L. Li, M. Zhou, H. Ding, Y. Yang, X. Li, K. Ding, DL-3-n-Butylphthalide (NBP) provides neuroprotection in the mice models after traumatic brain injury via Nrf2-ARE signaling pathway, Neurochem. Res. 42 (2017) 1375–1386.

[4] S. Prabhakaran, I. Ruff, R.A. Bernstein, Acute stroke intervention: a systematic review, JAMA 313 (2015) 1451–1462.

[5] X.Q. Chen, K. Qiu, H. Liu, Q. He, J.H. Bai, W. Lu, Application and prospects of butylphthalide for the treatment of neurologic diseases, Chin. Med. J. (Engl.) 132 (2019) 1467–1477.

[6] S. Wang, F. Ma, L. Huang, Y. Zhang, Y. Peng, C. Xing, Y. Feng, X. Wang, Y. Peng, Dl-3-n-Butylphthalide (NBP): a promising therapeutic agent for ischemic stroke, CNS Neurol. Disord.: Drug Targets 17 (2018) 338–347.

[7] N. Chen, Z. Zhou, J. Li, B. Li, J. Feng, D. He, Y. Luo, X. Zheng, J. Luo, J. Zhang, 3-n-butylphthalide exerts neuroprotective effects by enhancing anti-oxidation and attenuating mitochondrial dysfunction in an in vitro model of ischemic stroke, Drug Des. Dev. Ther. 12 (2018) 4261–4271.

[8] K. Itoh, T. Chiba, S. Takahashi, T. Ishii, K. Igarashi, Y. Katoh, T. Oyake, N. Hayashi, K. Satoh, I. Hatayama, M. Yamamoto, Y. Nabeshima, An Nrf2/small Maf heterodimer mediates the induction of phase II detoxifying enzyme genes through antioxidant response elements, Biochem. Biophys. Res. Commun. 236 (1997) 313–322.

[9] F. Sivandzade, S. Prasad, A. Bhalerao, L. Cucullo, NRF2 and NF-B interplay in cerebrovascular and neurodegenerative disorders: molecular mechanisms and possible therapeutic approaches, Redox Biol. 21 (2019), 101059.

[10] C. Lv, S. Maharjan, Q. Wang, Y. Sun, X. Han, S. Wang, Z. Mao, Y. Xin, B. Zhang, Alpha-lipoic acid promotes neurological recovery after ischemic stroke by activating the Nrf2/HO-1 pathway to attenuate oxidative damage, Cell. Physiol. Biochem. 43 (2017) 1273–1287.

[11] R.A. Linker, A. Haghikia, Dimethyl fumarate in multiple sclerosis: latest developments, evidence and place in therapy, Ther. Adv. Chron. Dis. 7 (2016) 198–207.

[12] Y. Chen, X. Zhang, Y. Yang, L. Zhang, L. Cui, C. Zhang, R. Chen, Y. Xie, J. He, W. He, Tert-butylhydroquinone enhanced angiogenesis and astrocyte activation by activating nuclear factor-E2-related factor 2/heme oxygenase-1 after focal cerebral ischemia in mice, Microvasc. Res. 126 (2019), 103891.

[13] U. Schulze-Topphoff, M. Varrin-Doyer, K. Pekarek, C.M. Spencer, A. Shetty, S.A. Sagan, B.A. Cree, R.A. Sobel, B.T. Wipke, L. Steinman, R.H. Scannevin, S.S. Zamvil, Dimethyl fumarate treatment induces adaptive and innate immune modulation independent of Nrf2, Proc. Natl. Acad. Sci. U. S. A. 113 (2016) 4777–4782.

[14] C. Zhang, Z. Zhang, Q. Zhao, X. Wang, H. Ji, Y. Zhang, (S)-ZJM-289 preconditioning induces a late phase protection against nervous injury induced by transient cerebral ischemia and oxygen-glucose deprivation, Neurotox. Res. 26 (2014) 16–31.

[15] X. Li, C. Ren, S. Li, R. Han, J. Gao, Q. Huang, K. Jin, Y. Luo, X. Ji, Limb remote ischemic conditioning promotes myelination by upregulating PTEN/Akt/mTOR signaling activities after chronic cerebral hypoperfusion, Aging Dis 8 (2017) 392–401.

[16] R. Saggu, T. Schumacher, F. Gerich, C. Rakers, K. Tai, A. Delekate, G.C. Petzold, Astroglial NF-kB contributes to white matter damage and cognitive impairment in a mouse model of vascular dementia, Acta Neuropathol. Commun. 4 (2016) 76.

[17] R.J. Franklin, C. Ffrench-Constant, Remyelination in the CNS: from biology to therapy, Nat. Rev. Neurosci. 9 (2008) 839–855.

[18] M. Li, N. Meng, X. Guo, X. Niu, Z. Zhao, W. Wang, X. Xie, P. Lv, Dl-3-n-Butylphthalide promotes remyelination and suppresses inflammation by regulating AMPK/SIRT1 and STAT3/NF-kappaB signaling in chronic cerebral hypoperfusion, Front. Aging Neurosci. 12 (2020) 137.

[19] S. Kuhn, L. Gritti, D. Crooks, Y. Dombrowski, Oligodendrocytes in Development, Myelin Generation and beyond, Cells (2019) 8.

[20] S. Love, Demyelinating diseases, J. Clin. Pathol. 59 (2006) 1151–1159.

[21] A. Saxena, J. Bauer, T. Scheikl, J. Zappulla, M. Audebert, S. Desbois, A. Waisman, H. Lassmann, R.S. Liblau, L.T. Mars, Cutting edge: multiple sclerosis-like lesions induced by effector CD8 T cells recognizing a sequestered antigen on oligodendrocytes, J. Immunol. 181 (2008) 1617–1621.

[22] I.D. Duncan, A.B. Radcliff, Inherited and acquired disorders of myelin: the underlying myelin pathology, Exp. Neurol. 283 (2016) 452–475.

[23] M. Bradl, H. Lassmann, Oligodendrocytes: biology and pathology, Acta Neuropathol. 119 (2010) 37–53.

[24] S.K. Chiang, S.E. Chen, L.C. Chang, A dual role of heme oxygenase-1 in cancer cells, Int. J. Mol. Sci. 20 (2018).

[25] L. Liu, M.G. Kelly, E.L. Wierzbicki, I.C. Escober-Nario, M.K. Vollmer, S. Dore, Nrf2 plays an essential role in long-term brain damage and neuroprotection of Korean red ginseng in a permanent cerebral ischemia model, Antioxidants (Basel) (2019) 8.

[26] G.S. Drummond, J. Baum, M. Greenberg, D. Lewis, N.G. Abraham, HO-1 overexpression and underexpression: clinical implications, Arch. Biochem. Biophys. 673 (2019), 108073.

[27] D. Bereczki Jr., J. Balla, D. Bereczki, Heme oxygenase-1: clinical relevance in ischemic stroke, Curr. Pharmaceut. Des. 24 (2018) 2229–2235.

[28] D. Ross, D. Siegel, Functions of NQO1 in cellular protection and CoQ10 metabolism and its potential role as a redox sensitive molecular switch, Front. Physiol. 8 (2017) 595.